(12) INTERNATIONAL APPLICATION PUBLISHED UNDER THE PATENT COOPERATION TREATY (PCT)

(19) World Intellectual Property Organization
International Bureau

(43) International Publication Date
6 November 2008 (06.11.2008)

PCT

(10) International Publication Number
WO 2008/132522 A1

(51) International Patent Classification:
A61B 5/00 (2006.01) *G01N 21/64* (2006.01)

(21) International Application Number:
PCT/HR2007/000013

(22) International Filing Date: 25 April 2007 (25.04.2007)

(25) Filing Language: English

(26) Publication Language: English

(71) Applicant *(for all designated States except US)*: **RUDER BOSCOVIC INSTITUTE** [HR/HR]; Bijenicka cesta 54, HR-10000 Zagreb (HR).

(72) Inventor; and
(75) Inventor/Applicant *(for US only)*: **KOPRIVA, Ivica** [HR/HR]; Domagojeva 12, HR-10000 Zagreb (HR).

(74) Agent: **KORPER ZEMVA, Dina**; Korper & Haramija, Prilaz Gjure Dezelica 16, HR-10000 Zagreb (HR).

(81) Designated States *(unless otherwise indicated, for every kind of national protection available)*: AE, AG, AL, AM, AT, AU, AZ, BA, BB, BG, BH, BR, BW, BY, BZ, CA, CH, CN, CO, CR, CU, CZ, DE, DK, DM, DZ, EC, EE, EG, ES, FI, GB, GD, GE, GH, GM, GT, HN, HR, HU, ID, IL, IN, IS, JP, KE, KG, KM, KN, KP, KR, KZ, LA, LC, LK, LR, LS, LT, LU, LY, MA, MD, MG, MK, MN, MW, MX, MY, MZ, NA, NG, NI, NO, NZ, OM, PG, PH, PL, PT, RO, RS, RU, SC, SD, SE, SG, SK, SL, SM, SV, SY, TJ, TM, TN, TR, TT, TZ, UA, UG, US, UZ, VC, VN, ZA, ZM, ZW.

(84) Designated States *(unless otherwise indicated, for every kind of regional protection available)*: ARIPO (BW, GH, GM, KE, LS, MW, MZ, NA, SD, SL, SZ, TZ, UG, ZM, ZW), Eurasian (AM, AZ, BY, KG, KZ, MD, RU, TJ, TM), European (AT, BE, BG, CH, CY, CZ, DE, DK, EE, ES, FI, FR, GB, GR, HU, IE, IS, IT, LT, LU, LV, MC, MT, NL, PL, PT, RO, SE, SI, SK, TR), OAPI (BF, BJ, CF, CG, CI, CM, GA, GN, GQ, GW, ML, MR, NE, SN, TD, TG).

Declaration under Rule 4.17:
— *of inventorship (Rule 4.17(iv))*

Published:
— *with international search report*
— *with amended claims and statement*

(54) **Title:** METHOD FOR REAL TIME TUMOUR VISUALISATION AND DEMARCATION BY MEANS OF PHOTODYNAMIC DIAGNOSIS

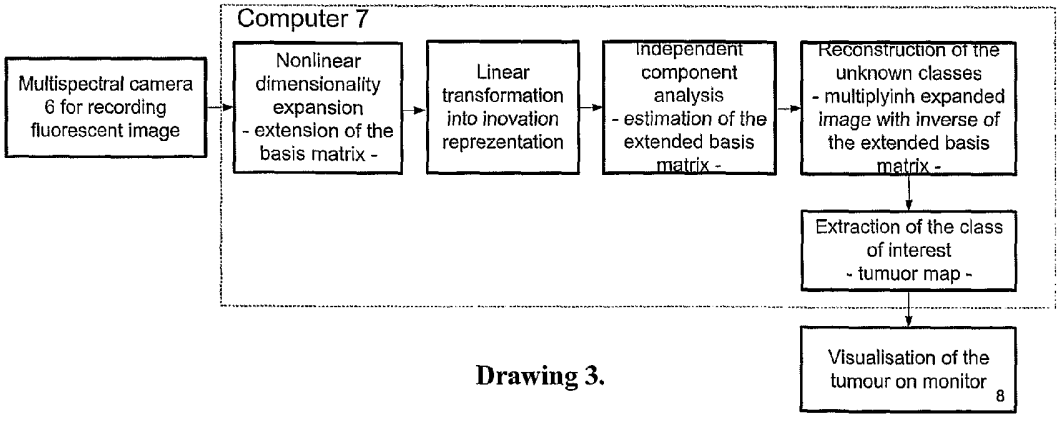

Drawing 3.

(57) **Abstract:** Proposed invention is related to the field of photodynamic therapy and photodiagnosis. Specifically, a new algorithm is presented for visualisation and spatial demarcation of various types of tumours and unhealthy tissue through unsupervised segmentation of the fluorescent multispectral image. Image is acquired through recording of the emission of the tissue illuminated by the light that induces fluorescence in the tumour. For this purpose tissue is treated by photo sensitizer. Algorithm for real time visualisation and spatial demarcation of the tumour by means of the analysis of fluorescent image consists of the recording of the fluorescent image (1) that represents linear combination of the unknown classes S by multispectral camera, transformation of the fluorescent multispectral image into new multispectral image (2) applying nonlinear dimensionality expansion, linear transformation of the multispectral image (2) with extended dimensionality, independent component analysis of the innovation representations of the multispectral image (3) that is result of the transformation of the fluorescent image (1) and multispectral image (2), extraction o the tumour map or class of interest in accordance with the chosen criterion and visualisation of tumour on monitor.

WO 2008/132522 A1

Method for real time tumour visualisation and demarcation by means of photodynamic diagnosis

TECHNICAL FIELD

[0001] Proposed invention is related to the field of photodynamic therapy and photodiagnosis. Specifically, the invention is related to the novel method for visualisation and spatial demarcation of the various types of tumours i.e. unhealthy tissues by means of unsupervised segmentation of the fluorescent multispectral image. The image is obtained by acquiring emission of the fluorescence of the illuminated tissue. For this purpose the tissue is treated by photo sensitizer. As an example we mention δ-5-aminolaevulinic acid (ALA), with the ability to induce a fluorophore such as protoporphyrin IX (Pp IX) which has a capability of auto-fluorescence when illuminated with the light of a specific wavelength. More detailed description of the photo sensitizers used to induce fluorophores in the tumour tissue is given in the state-of-the-art, paragraphs [0003] - [0006].

STATE OF THE ART

[0002] Existing systems for visualisation and demarcation of tumours are based on visualisation of fluorophores accumulated in the tumour tissue by means of the system for the acquisition of the fluorescent image. Fluorescent image can be obtained in various ways depending on the properties of the chosen fluorophore. The basis for the successful visualisation of the tumour is increased concentration of the fluorophore in the tumour tissue that is achieved after few hours of the treatment by photo sensitizer.

[0003] Example that is often used for the photo sensitizer is δ-5-aminolaevulinic acid (ALA). It induces Pp IX which has ability of selective fluorescence in the wavelength interval between 600nm and 700nm after being illuminated by 405nm. (Koenig F, Knittel J, Stepp H. Diagnostic Cancer in Vivo. Science 2001; 292: 1401-1403; Bäumler W, Abels C, Szeimies RM. Fluorescence Diagnosis and Photodynamic Therapy. Dermatology. Med. Laser Appl. 2003; 18:47-56.). As an example, by using this fluorophore and device schematically shown

in Figure 1, that consists of the light illuminator, CCD camera and computer, it is possible to visualise various types of the skin tumours.

[0004] For the purpose of the visualisation of the tumour on the cell level nano-particles are used as fluorescent markers. An example is green fluorescent protein with the ability to label tumour cells through the mechanism of selective bonding. (Hasegawa S, Yang N, Chishima T, Miyagi Y, Shimada H, Moossa A. R., Hoffman M. R. In vivo tumor delivery of the green fluorescent protein gene to report future occurence of metastasis. Caner Gene Therapy 2000; 10: 1336-1340; R. M. Hoffman. Green fluorescent protein imaging of tumor growth, metastasis, and angiogenesis in mouse models. The Lancet Oncology 2002; 3: 546-556.)
By combining such cell markers and device schematically shown in Figure 2, that consists of endoscope, fluorescent microscope, CCD camera and computer, it is possible to visualise a tumours of the lung, prostate, stomach, liver, brain, lymph nodes, bone, pancreas, colon, etc.

[0005] For the purpose of the visualisation of the brain tumour nano-particle CLIO-Cy5.5 is used as a fluorescent marker. Simultaneously, it is used as a contrast agent for magnetic resonance imaging and fluorescent agent for near infrared imaging. This agent enables recording of the multimodal image of the brain through combination of the magnetic resonance image and near infrared fluorescent image. Application of the nano-particle CLIO-Cy5.5 in visualisation of the brain tumours is described in: Tréhin R, Figueiredo J. L., Pittet M. J., Weissleder R., Josephson L, Mahmood U. Fluorescent Nanoparticle Uptake for Brain Tumor Visualization. Neoplasia 2006; 4: 302-311.

[0006] Multimodal imaging is also used for the purpose of the visualisation of the surface tumours on small animals. An example includes combination of the fluorescent optical image and radio image recorded by gamma camera. Hematoporphyrin is used as photo sensitizer to generate fluorescent optical image while radio-marker Tc-99m is used to generate radio image. Such system is described in: Autiero M., Celentano L, Cozzolino R, , Marotta M, Mettivier G, Montesi M.C., Riccio P, Roberti G, Russo P. Experimental Study on In Vivo Optical and Radionuclide Imaging in Small Animals. IEEE Trasactions on Nuclear Science 2005; 52: 205-209; Celentano L, Laccetti P, Liuzzi R, Mettivier G, Montesi M. C., Autiero M., Riccio P, Roberti G, Russo P. Preliminary Tests of a Prototype System for Optical and

Radionuclide Imaging in Small Animals. IEEE Trasactions on Nuclear Science 2003; 50: 1693-1701.

[0007] One of the methods used to calculate tumour demarcation line by visualisation of the Pp IX is the *ratio imaging* method: Scott MA, Hopper C, Sahota A, Springett R, Mcllroy BW, Bown SG, MacRobert AJ. Fluorescence Photodiagnostics and Photobleaching Studies of Cancerous Lesions using Ratio Imaging and Spectroscopic Techniques. Lasers Med Sci 2000; 15:63-72. The method calculates ratio between intensity of the red component of the RGB image (600 to 700 nm) and intensity of the green component if the RGB image (450 to 550 nm). Thus, visual contrast between tumour and healthy tissue is greatly enhanced. Let the image obtained by this method be denoted as: RG=R/G. Dynamic ratio of the RG image is large due to the fact that division operation involves division with very small numbers. In order to preserve contrast of the RG image a threshold is introduced. Intensities of all the pixels in RG image with a value greater than a threshold value are made equal to the threshold value. This is a serious disadvantage of the ratio imaging method because the optimal threshold value is highly dependent on the intensity of the fluorescence. Because of that the ratio imaging method is highly sensitive on the variation of the fluorescence intensity level. A various reasons can lead to this variation: variability of the time interval of the tumour administration by means of photo sensitizer, variability of the intensity of illuminating light, as well as variability of the sensitivity of the image acquisition system. Described sensitivity can significantly influence accuracy of the tumour demarcation by means of the ratio imaging method. As it will be described one of the important features of the proposed invention is robustness with respect to the variation of the intensity level of the fluorescent image.

[0008] Yet another method for the spatial demarcation of the tumour by visualisation of Pp IX is the *optimal threshold method*: Ericson MB, Sandberg C, Gudmundson F, Rosén A, Larkö O, Wennberg AM. Fluorescence contrast and threshold limit: implications for photodynamic diagnosis of basal cell carcinoma in Journal of Photochemistry and Photobiology B: Biology 2003; 69: 121-127. This method classifies as a tumour areas of the fluorescent image with the intensity level greater than the value set by the threshold. The threshold is defined as a value of the average intensity level corrected by an appropriate factor. It has been empirically found that the correction factor varies between 1.4 and 1.6 if the treatment of the tumour with ALA is between three and four hours. Such imprecision in setting the threshold influences

significantly the accuracy of the spatial demarcation of the tumour by means of the optimal threshold method.

[0009] Yet another technique frequently used for tumour demarcation is based on the calculation of the difference image obtained by subtracting two or more images recorded in response to the various illuminations. Quite often difference image is superimposed on the image obtained as response on the illumination by white (polychromatic) light. For example in: Fischer F, Dickson EF, Pottier RH, Wieland H. An Affordable, Portable Fluorescence Imaging Device for Skin Lesion Detection Using a Dual Wavelength Approach for Image Contrast Enhancement and Aminolaevulinic Acid-induced Protoporphyrin IX. Part. I. Design, Spectral and Spatial Characteristics. Lasers Med Sci 2001; 16:199-206, a procedure has been described that superimposes difference image, obtained by illuminations with two monochromatic lights, on an image obtained by illumination with polychromatic light. In principle this type of methods has an increased sensitivity on the variability of the image intensity level what has significant influence on the accuracy of the demarcation. In order to produce spatial tumour map with good visual contrast the image difference methods require high intensity level of the illuminating light. Method proposed in the invention has two advantages in relation to the image difference methods only one illumination is required; accuracy of the demarcation is significantly increased because the method is approximately invariant in relation to the variability of the intensity level of the acquired fluorescent image. Thus, the proposed invention enables estimation of the accurate spatial map of the tumour even when the intensity level of the illuminating light is reduced.

[0010] System for the real time acquisition of the image of the brain tumour is described in the patent US6161031 (B2). System combines frame difference and frame averaging methods with the super-positions on the standard image of the tumour. The goal is to enable a neuro-surgeon to obtain accurate tumour demarcation during the surgery. Regarding the accuracy of this image acquisition methods and advantages of the method proposed in the invention, the same comments applied as in paragraph [0009].

[0011] Image difference method is also used in the patent US5845639 (B2), where a procedure for tumour localisation is based on measuring the oxygen level in the blood. Tissue is illuminated by electromagnetic radiation in visible or infrared part of the spectrum. Spatial

map of the tumour is obtained by subtracting reference image (acquired without illumination) from the image obtained as response to illumination. Regarding the accuracy of this image acquisition methods and advantages of the method proposed in the invention, the same comments applied as in paragraphs [0009] and [0010].

[0012] Similarly as in [0009], [0010] and [0011] in the patent application US2006004292 (A1) a real time tumour demarcation method is described. The method is based on the difference between images acquired under illumination with polychromatic and monochromatic light and superimposing difference image onto polychromatic image. Regarding the accuracy of this image acquisition methods and advantages of the method proposed in the invention, the same comments applied as in paragraphs [0009], [0010]. and [0011].

[0013] In the document WO 96/14795 yet another system is protected that detects solid tumours in real time, including possibility of gradation and characterization of the tumour tissue. The system includes image processing method that combines frame difference and frame averaging methods by superposition of the difference image on the standard image of the tumour. The same comments apply as for the method described in paragraph [0009]. Frame difference and frame averaging methods work well if the contrast agent i.e. photo sensitizer is used in an appropriate concentration, in the appropriately long time interval and if the intensity of the illuminating light is high enough. The method proposed in this invention has the property of generating spatial map of the tumour with a good visual contrast when the intensity level of the fluorescent image is fluctuating.

[0014] In the document WO 93/25141 yet another system is protected that calculates demarcation line and dimensions of the solid tumour tissue in the region of interest. The region of interest is illuminated by the light with high intensity and wavelength that is absorbed by the fluorophore accumulated in the increased concentration in the tumour tissue. The image processing is still based on the averaging of the control image used to form a difference image. In order to increase a visual contrast of the spatial map of the tumour this method additionally assumes illumination with at least two wavelengths. As already commented, the image processing algorithms are quite primitive and based on frame difference and frame averaging. Therefore, it is required that intensity of the illuminating light

be high enough, that photo sensitizer be applied with the appropriate concentration and during the time interval that is long enough. Method proposed in the invention has the property to ensure the spatial map of the tumour with a visual contrast the quality of which is in principle not critically dependent from the level of intensity of illuminating light, as well as from the level of the concentration and duration of treatment by the photo sensitizer. In addition to that, the proposed method assumes the tissue illumination in the region of interest by only one wavelength. This significantly simplifies realisation of the photodynamic and photodiagnoses system. (instead of two only one laser is used to illuminate the tissue).

[0015] In the patent application US20050280813 a method is described that enhances the visual contrast on the image during tumour detection i.e. cytological examinations. The method superimposes images of the tissue in visible and infrared parts of the spectrum, where the fact is used that infrared light is significantly more sensitive on molecular and biochemical variations what represents the basis for tumour detection. Method proposed in the invention requires significantly simplified realisation of the system for photo-dynamic therapy due to the fact that for the purpose of the analysis only image in the visible part of the spectrum has to be used.

[0016] In the patent US5865754 (B2) an optical system is described that is used for non-invasive tumour detection by combining tissue illumination with modulated light and acquisition of the fluorescent image as a response on the illumination. Spatial map of the fluorescence is obtained as a solution of the diffusion equation in the frequency domain. The method proposed in the invention is similar to this method only due to the fact that induced fluorescence is used as a basis for the image processing that yield a spatial map of the tumour. The difference is twofold: proposed method does not require illumination with the modulating light and because of that the system for photodynamic therapy is simpler for realisation; the image processing method used to obtain a spatial map of the tumour is geometric-statistical by nature and enables generation of the spatial map of the tumour as a solution of the problem of unsupervised segmentation of the fluorescent multispectral image.

[0017] In the patent US5784162 (B2) a system for localisation of the biological structures, including the skin tumours, is described. It combines spectroscopy, CCD imaging system and algorithms for the multispectral image analysis. For the purpose of the image segmentation an

algorithm is used that is based on the similarity principle. This algorithm assumes that is possible to localize a pixel that contains the pure class i.e. tumour. The remaining pixels are then classified based on similarity with a reference pixel, where the criterion for similarity is an angle between the two spectral vectors. This algorithm belongs to the class of supervised classification methods and is already in use for classification of airborne and spaceborne multispectral and hyperspectral images. The algorithm is characterized by significant errors in classification of spectrally similar classes, especially when the spectral resolution is poor. Such case can be expected in the early stage of tumour development when recorded by a multispectral camera. Then, spectral characteristic of the tumour is similar to the spectral characteristic of the surrounding healthy tissue. Method proposed in the invention is robust in relation to such conditions.

[0018] In the patent application US20060200318 (A1) a method is described that is based on the independent component analysis. It is used to separate reflections of the illuminating radiation from the fluorescence in the systems with multiple fluorescence, where the fluorescence from one illumination is superimposed on the reflection from another illumination. By method proposed in the invention that combines nonlinear dimensionality expansion, innovations representation and independent component analysis, it is possible in principle to enhance the level of suppression of the reflected illuminating radiation, because it is spectrally similar (statistically dependent) with a fluorescence.

[0019] Tumour demarcation can be also achieved by using methods for supervised and unsupervised segmentation of the fluorescent multispectral image.

[0020] Methods for supervised segmentation classify multispectral image in relation to the reference spectral response of the tumour. Accuracy of this approach is significantly limited by the variability of spectral responses of the tumour and healthy tissue. This is especially the case when the spectral resolution is poor, what is the case with an RGB image. One method for supervise segmentation is already discussed spectral similarity method as described in paragraph [0017].

[0021] Unsupervised segmentation methods classify multispectral image through looking for extremes of the functional that is a measure of the some of the features for which it is known

to represent a class of interest. One of the most successful methods in this domain is independent component analysis (ICA). ICA methods belong to group of statistical methods for unsupervised or blind solution of linear and nonlinear inverse problems. Unsupervised segmentation of the multispectral image belongs to this group of problems. Application of the ICA methods to the problem of unsupervised segmentation of the hyperspectral image is for example described in: Q. Du, I. Kopriva, H. Szu. Independent Component Analysis for Hyperspectral Remote Sensing. Optical Engineering; vol. 45: 017008-1-13, 2006; and also in the patent US6944571 (B2).

[0022] Assumptions upon which the ICA algorithms are built are that unknown classes are statistically independent and non-Gaussian, as well as that the number of linearly independent columns of the unknown basis matrix is greater or equal to the number of classes. One of the most known ICA algorithms is described in the patent US5706402 (B2), patent application WO 9617309 (A), as well as in the paper: A. J. Bell and T. J. Sejnowski. An information-maximization approach to blind separation and blind deconvolution. Neural Computation; vol. 7, pp.1129-1159, 1995. Reference literature for the field of blind source separation and independent component analysis is: A. Hyvärinen, J. Karhunen, E. Oja. *Independent Component Analysis*, John Wiley, 2001; A. Cichocki, S. Amari. *Adaptive Blind Signal and Image Processing*, John Wiley, 2002. Advantage of the ICA algorithms in relation to the state-of-the-art methods for tumour demarcation described in paragraphs [0008]-[0017], is in their invariance with respect to the variability of the intensity level of the image. This is a consequence of the fact that statistical independence is invariant with respect to the amplitude of the stochastic process.

[0023] Statistical independence assumption is however not correct for spectrally similar classes. This is especially the case with the low-dimensional multispectral image with the poor spectral resolution, such as RGB image. Another consequence of the spectrally similar classes is that the unknown basis matrix is badly conditioned i.e. the columns of the basis matrix associated with the spectrally similar classes are linearly dependent. Because of that direct application of the ICA algorithms to unsupervised segmentation of the multispectral image produces inaccurate tumour demarcation.

[0024] Problem of blind separation of statistically dependent classes is quite often in biomedical field as for example in the analysis of the EEG signals and analysis of gene microarrays. Because of that in the patent US6728396 (B2) it is protected an algorithm for blind separation of blind separation of statistically dependent signals that can even be Gaussian. The basis of the algorithm is identification of the set of measurements where source signals are statistically independent. The unknown basis matrix is then identified by some of the standard ICA algorithms (the FastICA algorithm has been used in the patent) on the set of selected measurements. Criterion used to identify the set of measurements with statistically independent signals is of the *ad hoc* type and specific for the gene sequence analysis in molecular biology. This is a field where the algorithm is applied. In addition to the fact that identification of the set of measurements with statistically independent processes reduces the effective number of measurements, what influences the accuracy of the ICA algorithms, another disadvantage of this patented algorithm is that its application is limited to the gene sequence analysis.

[0025] In references: A. Cichocki, P. Georgiev. Blind source separation algorithms with matrix constraints. IEICE Transactions on Fundamentals of Electronics, Communications and Computer Sciences; *E86-A*, 522-531, 2003; A. Cichocki. General Component Analysis and Blind Source Separation Methods for Analyzing Multichannel Brain Signals; Statistical and Process Models of Cognitive Aging, Notre Dame Series on Quantitative Methods, Editors: M.J Wenger and C. Schuster. Mahwah, NJ: Erlbaum, 2007; T. Tanaka, A. Cichocki. Subband decomposition independent component analysis and new performance criteria. Proc. IEEE Int. Conf. on Acoustics, Speech and Signal Processing (ICASSP 2004), Montreal, Canada, 2004, pp. 541-544; some of the algorithms for blind separation of statistically dependent signals are described. These algorithms differ by accuracy and computational complexity but have in common that in a case of statistically dependent processes produce more accurate results than those obtained by direct application of the ICA algorithms. We mention again that unsupervised segmentation of the multispectral image belongs to the class of problems with statistically dependent signals.

[0026] Main characteristic of the algorithms for blind separation of statistically dependent signals is that by means of some transformation the original data set is transformed in the new data set where transformed unknown classes are less statistically dependent. The condition

that has to be fulfilled is that the unknown basis matrix in the linear mixture model has to invariant with respect to the transform. This enables more accurate estimation of the basis matrix by application of the ICA algorithms on a transformed data. On this way the scale invariance is preserved i.e. the segmentation method preserves robustness with respect to the variability of the intensity level of the fluorescent image. This represents the basis for the robustness of the tumour demarcation method in relation to the variability in duration of the treatment by photo sensitizer as well as in relation to the variability of the intensity of illuminating light.

[0027] In a case of segmenting low-dimensional multispectral image in addition to have statistically dependent classes there is a problem of spectral similarity between the classes. For example, this is the case in the early phase of the tumour development or when the intensity level of the fluorescence is low. Consequence of the spectral similarity is that corresponding column vectors of the basis matrix, that represent spectral responses of the classes, become linearly dependent. Nonlinear transformation of the multispectral image produces new image with increased dimensionality. Increased dimensionality is a result of the new nonlinearly generated spectral measurement that mutually linearly independent. Thus, consequence of the increased dimensionality is that classes in transformed image are spectrally less similar i.e. corresponding column vectors in the unknown basis matrix are linearly more independent. Application of this method to the problem of unsupervised segmentation of low-dimensional remotely sensed multispectral image is described in: H. Ren, C. I. Chang. A Generalized Orthogonal Subspace Projection Approach to Unsupervised Multispectral Image Classification. IEEE Transactions on Geoscience and Remote Sensing; vol. 38, No. 6, November 2000, pp. 2515-2528; Q. Du, I. Kopriva, H. Szu. Independent Component Analysis for Classifying Multispectral Images with Dimensionality Limitation. International Journal of Information Acquisition; Vol. 1, No. 3, 2004, pp. 201-215.

[0028] Generalization of the nonlinear dimensionality expansion technique described in the state-of-the-art paragraph [0027], are the ICA algorithms in the so called kernelised version. First formulation of the kernel ICA method has been given in: Francis R. Bach, Michael I. Jordan. Kernel Independent Component Analysis, Journal of Machine Learning Research, 3, 1-48, 2002. Most important characteristic of this approach is that ICA algorithms are applied

on nonlinearly transformed multispectral image in a new high-dimensional space. In principle, this enables more accurate segmentation of the spectrally similar classes.

DETAILED DESCRIPTION OF THE INVENTION

[0029] Proposed invention is related to the field of photodynamic therapy and photodiagnosis. More specific, the invention is related to the new method for visualisation and demarcation of the various types of tumours and unhealthy tissue by means of unsupervised segmentation of the fluorescent multispectral image. The case of under-surface tumours is related to the tumours of lung, prostate, stomach, liver, brain, lymph nodes, spine, etc. They are visualised on the cell level by means of green fluorescent protein gene that is used as a fluorescent marker and has ability to bond selectively on tumour cells. When visualising under-surface tumours it is assumed that visualisation device consists of endoscope, fluorescent microscope and multispectral camera. When the intensity level of the fluorescent image is varying especially good visual contrast of the spatial map of the surface tumours is obtained by combined use of the method of nonlinear dimensionality expansion of the multispectral image 1, linear transformation of the multispectral of the multispectral image 2 into innovations representation 3, and applying independent component analysis on the innovations representation 3.

[0030] The invention is related to the real time visualisation and demarcation of tumours by unsupervised segmentation of the fluorescent multispectral image 1 by means of the algorithms for nonlinear dimensionality expansion and algorithms for blind separation of statistically dependent processes.

BRIEF DESCRIPTION OF DRAWINGS

In the sequel a more detailed description of the invention will be given with references to the following drawings:

- drawing 1 schematically illustrates block diagram of the device for the visualisation of the surface tumours through the analysis of the multispectral fluorescent image,

- drawing 2 schematically illustrates block diagram of the device for the visualisation of the sub-surface tumours through the analysis of the multispectral fluorescent image,
- drawing 3 schematically illustrates block diagram of the approach for unsupervised segmentation of the multispectral fluorescent image and obtaining spatial map of the surface and sub-surface tumours with a good visual contrast,
- drawings 4A and 4B schematically illustrate spectral similarity between the classes $\mathbf{s}_1$ and $\mathbf{s}_2$ in appropriate spatial visualisation,
- drawing 5 schematically illustrates spectrally similar and spectrally different classes $\mathbf{s}_1$ and $\mathbf{s}_2$ in the wavelength region,
- drawing 6 schematically illustrates spectrally similar and spectrally different classes $\mathbf{s}_1$ and $\mathbf{s}_2$ in appropriate coordinate systems,
- drawing 7 schematically illustrates quality of the spatial map of the healthy tissue $\mathbf{s}_1$ and tumour $\mathbf{s}_2$ which are extracted by direct application of the ICA algorithms to two-spectral image 4A,
- drawing 8 schematically illustrates quality of the spatial map of the healthy tissue $\mathbf{s}_1$ and tumour $\mathbf{s}_2$ which are extracted by application of the ICA algorithms on multispectral image obtained after nonlinear dimensionality expansion and linear transform that yields innovations representation, to two-spectral image 4A.
- drawings 9A and B respectively shows tumour with the high level of the fluorescence and the same tumour with the low level of the fluorescence.
- drawings 10A and B respectively shows demarcation lines of the tumours shown on drawings 9A and 9B which are described by described invention that combines nonlinear dimensionality expansion, innovations representations and independent component analysis,
- drawings 11A and B respectively shows demarcation lines of the tumours shown on drawings 9A and 9B which are extracted by the ratio imaging method with a threshold value set to 5 in accordance to the existing state-of-the-art, and
- drawings 12A and B respectively shows demarcation lines of the tumours shown in drawings 9A and 9B which are extracted by the ratio imaging method with a threshold value set to 10 in accordance with the existing state-of-the-art.

[0031] Schematic block diagram of the device for the visualisation of the surface tumours through segmentation of the multispectral fluorescent image 1 is shown in drawing 1. The device consists of: light source 4 used to illuminate the surface tissue 5 with the purpose to induce fluorescence; multispectral camera 6 with the purpose to record fluorescent image of the illuminated surface tumour; computer 7 where algorithms for unsupervised segmentation of the multispectral fluorescent image are implemented; monitor 8 used to display the spatial map of the surface tumours.

[0032] Schematic block diagram of the device for the visualisation of the sub-surface tumours through segmentation of the multispectral fluorescent image 1 is shown in drawing 2. The device consists of: endoscope 10 used to illuminate tissue of interest 9 with the aim to induce fluorescence and transfer image to microscope 11; multispectral camera 6 used to record magnified image of the illuminated sub-surface tissue; computer 7 where algorithms for unsupervised segmentation of the multispectral fluorescent image are implemented; monitor 8 used to display the spatial map of the surface tumours.

[0033] Procedure for processing multispectral fluorescent image with the aim to extract and visualise spatial map of the tumour with a good visual contrast is implemented in the software in the computer 7 and consists of the following steps schematically shown in drawing 3: recorded multispectral image 1 is transformed by nonlinear dimensionality expansion transform into new multispectral image with the aim to increase spectral dissimilarity among the classes; multispectral image with increased dimensionality 2 is transformed by linear transform with the aim to increase statistical independence among the unknown classes yielding as a result innovations representation of the multispectral fluorescent image 3; independent component analysis algorithms are applied on innovations representation of the multispectral image in order to estimate extended basis matrix $\overline{\mathbf{A}}$; as a final result it is estimated the matrix of the unknown classes **S** among which there is a spatial map of the tumour with enhanced visual contrast which is extracted according to the chosen criteria and displayed on monitor 8.

[0034] Procedure for real time visualisation and demarcation of the tumours using photodynamic method and segmentation of the fluorescent multispectral image consist of the following steps:

- recording multispectral fluorescent image 1 with multispectral camera 6, where multispecral image is defined as a product of the unknown basis matrix **A** and matrix of the unknown classes **S**,
- transforming fluorescent multispectral image 1 into new multispectral image 2 by means of the nonlinear dimensionality expansion, where multispectral image 2 is defined as a product of the extended basis matrix $\overline{\mathbf{A}}$ and matrix of the unknown classes **S**,
- linear transformation of the multispectral image 2 with extended dimensionality into innovations representation of the multispectral image 3 defined as a product of the extended basis matrix $\overline{\mathbf{A}}$ and innovations representation of the matrix of the unknown classes $\widetilde{\mathbf{S}}$,
- estimation of the extended basis matrix $\overline{\mathbf{A}}$ or its inverse $\overline{\mathbf{A}}^{-1}$ by applying algorithms of the independent component analysis on innovations representation of the multispectral image (3),
- estimation of the matrix of unknown classes **S** through multiplication of the estimated inverse of the extended basis matrix $\overline{\mathbf{A}}^{-1}$ and multispectral image 2,
- extraction of the spatial map of the tumour or class of interest in accordance with the chosen criteria, and
- displaying the tumour on monitor 8.

[0035] Problem of the unsupervised segmentation of the multispectral image 1 by means of the ICA algorithms can algebraically be expressed as a matrix factorization problem $\mathbf{X} \in \mathbf{R}_{0+}^{m \times N}$ by means of which multispectral image 1 is represented:

$$\mathbf{X} = \mathbf{AS} \qquad [1]$$

In equation [1] **X** represents multispectral image 1 where $\mathbf{A} \in \mathbf{R}_{0+}^{m \times n}$ represents unknown basis matrix and $\mathbf{S} \in \mathbf{R}_{0+}^{n \times N}$ represents matrix of the unknown classes. In adopted notation m represents number of spectral components of the multispectral image, N represent number of pixels of the multispectral image, and n represents number of the unknown classes. Unsupervised segmentation methods estimate the unknown basis matrix **A** and unknown class matrix **S** using only the data matrix **X** and some *a priori* information about the classes. ICA

algorithms assume that unknown classes are mutually statistically independent and non-Gaussian, as well as that number of linearly independent column vectors of the basis matrix is greater or equal to the number of unknown classes. These assumptions suffice to reconstruct the unknown classes by means of the ICA algorithms and multisepctral image 1.

[0036] When multispectral image 1 is an RGB image the number of spectral components used in the representation described in paragraph [0035] is m=3. Number of unknown classes n contained in multispectral image 1 has to be estimated. One of the techniques used for this purpose is based on counting singular values of the data covariance matrix $\mathbf{R}_{xx} = (1/N)\mathbf{X}\mathbf{X}^{T}$, that are greater than threshold value defined by the signal-to-noise ratio. If there exists some *a priori* knowledge about the image scene it is possible to set the number of the unknown classes n in advance. For example, if the image of the skin tumour is recorded it is logical to assume existence of the two classes in the image: tumour and healthy tissue. In such a case it follows n=2. Depending on the complexity of the scene this number can be increased. For example if the tumour on the head is imaged, the hair can also be one class in which case number of classes n should be set to 3.

[0037] In a case of the segmentation of the multispectral image 1 model defined by equation [1] has the following interpretation. Let m be number of spectral components. Let $\mathbf{x}$ be column vector $m\times1$ in multispectral image 1 and let it represent pixel in the multispectral image. Element x_i is intensity recorded on the ith wavelength. Base matrix $\mathbf{A}$ contains n spectral responses of the unknown classes i.e. $\mathbf{A}=[\mathbf{a}_1\ \mathbf{a}_2\ \ldots\ \mathbf{a}_n]$. Let $\mathbf{s}$ be unknown column vector $n\times1$ in the class matrix $\mathbf{S}$, that is associated $\mathbf{A}$, and that has to be estimated. Then s_i represents contribution of the class with spectral response $\mathbf{a}_i$ in the pixel $\mathbf{x}$. When $\mathbf{A}$ is known estimation of $\mathbf{s}$ is achieved by means of the least squares method. This is supervised segmentation. In the real world applications in medicine, agriculture and remote sensing it is difficult to known in advance spectral responses of the classes that are resident in the multispectral image 1. Thus, the case with the unknown basis matrix $\mathbf{A}$ is quite common in practice. When $\mathbf{A}$ is unknown the segmentation problem i.e. estimation of $\mathbf{s}$ becomes considerably more difficult and is known under automated or unsupervised segmentation. When two classes are identical the corresponding column vectors of the unknown basis matrix $\mathbf{A}$, which represent spectral responses of the appropriate classes, are parallel i.e. linearly dependent. Consequently, condition set in paragraph [0035], number of linearly

independent column vectors of the base matrix is greater or equal to the number of the unknown classes n , is not fulfilled. In addition to that, when the two classes are similar, for example tumour in the early phase of development is similar to the surrounding healthy tissue, corresponding column vectors of the unknown basis matrix **A** are almost parallel. Unsupervised segmentation of such multispectral images is a challenge for the algorithms and direct application of the ICA algorithms on multispectral image 1, in a case when it contains spectrally similar classes, does not produce an accurate result. Similar problem of the inaccurate segmentation also appears when the unknown number of classes n contained in the multispectral image is greater than the number of spectral components m in the multispectral image 1.

[0038] The purpose of the use of the algorithms for the nonlinear dimensionality expansion and blind separation of statistically dependent sources is that in combination with the ICA algorithms increase accuracy of the unsupervised segmentation of the multispectral image 1 when tumour and healthy tissue spectrally similar. This can be expected in the early phase of tumour development or when the multispectral image is low-dimensional. Drawings 4, 5 and 6 schematically illustrate effect of the mentioned algorithms in the segmentation of the spectrally similar classes.

[0039] According to the references cited in paragraph [0027] algorithm for nonlinear dimensionality expansion of the multispectral image can be described in the following way. Idea upon which algorithm for nonlinear dimensionality expansion is built follows from the assumption that the second order stochastic process is characterized by the statistics of the first and second order. When spectral images $\mathbf{x}_i$, i=1,..m, that represent row vectors of the multispectral image 1, are interpreted as the first order statistics it is then possible to generate the spectral images of the second order. They encompass linear and nonlinear correlations and cross-correlations contained in the multispectral image 1. Let $\{\mathbf{x}_i\}_{i=1}^{m}$ be the set of the first order spectral images. First set of the spectral images of the second order is possible to obtain on the basis of autocorrelations. They are constructed multiplying each spectral image by itself $\{\mathbf{x}_i^2\}_{i=1}^{m}$. Second set of the spectral images of the second order is constructed on the basis of cross-correlations between all spectral images of the first order $\{\mathbf{x}_i\mathbf{x}_j\}_{i,j=1,i\neq j}^{m}$. In overall this

yields $2m+\binom{m}{2}$ of the spectral images. For example if the multispectral image 1 is an RGB image with m=3 then described method of nonlinear dimensionality expansion transforms RGB image into new multisepctral image with m=9 spectral bands. In this new higher-dimensional space classes that in original RGB resolution were similar become less similar. Let us denote multispectral image with expanded dimensionality 2 as $\overline{\mathbf{X}}$. Acccording to definition it is a product of the extended basis matrix $\overline{\mathbf{A}}$ and matrix of the unknown classes **S**

$$\overline{\mathbf{X}} = \overline{\mathbf{A}}\mathbf{S} \qquad [2]$$

According to the explanation given in paragraph [0037] corresponding column vectors of the extended basis matrix $\overline{\mathbf{A}}$ become less collinear i.e. number of linearly independent column vectors of the extended basis matrix $\overline{\mathbf{A}}$ is greater than number of linearly independent column vectors of the basis matrix **A.** Thus, one of the basic conditions for successful application of the ICA algorithms to unsupervised segmentation of the multispectral image is fulfilled. If the dimensionality of the multispectral image 1 has to be increased further another set of the nonlinearly correlated spectral image can be generated as $\left\{\sqrt{\mathbf{x}_i}\right\}_{i=1}^{m}$.

[0040] As explained in the existing state-of-the-art, paragraph [0035], ICA algorithms assume that unknown classes are mutually statistically independent and non-Gaussian. In many practical situations, for example in a case of biomedical signals, these assumptions are not completely true. One of them is the assumption about statistical independence between the classes. Important references that cover problem of the unsupervised segmentation of the statistically dependent classes are cited in the paragraph [0025]. The challenge is to find a linear operator T with the property

$$T\left[\overline{\mathbf{X}}\right] = T\left[\overline{\mathbf{A}}\mathbf{S}\right] = \overline{\mathbf{A}}T\left[\mathbf{S}\right] \qquad [3]$$

such that transformed classes T[**S**] are more statistically independent than classes **S**. The unknown expanded basis matrix $\overline{\mathbf{A}}$ is estimated by applying ICA algorithms to the linearly transformed multispectral image 3. Some of the methods used to implement the linear

operator T are fixed and adaptive filter banks. Alternative to the filter banks is the use of innovations representation of the multispectral image 2 and that is proposed in the invention. Use of innovations representation as a linear transform T in order to enhance accuracy of the standard ICA algorithms has been suggested for the first time in : Hyvärinen, A. Independent component analysis for time-dependent stochastic processes. Proc. Int. Conf. on Artificial Neural Networks ICANN'98, 541-546, Skovde, Sweden, 1998. Important property of the innovations representations $T[\mathbf{S}]$ is that they are always more statistically independent and more non-Gaussian than classes **S**. These are the two fundamental conditions that have to be fulfilled for the ICA algorithms in order for them to yield accurate results when applied to segmentation of the multispectral image. Linear transform $T[\mathbf{S}]$ used to realize innovations representation T of the unknown classes $\mathbf{s}_i$, $i=1,\ldots,n$ is

$$\tilde{\mathbf{s}}_i(t) = \mathbf{s}_i(t) - E\left[\mathbf{s}_i(t) \middle| t, \mathbf{s}_i(t-1)\right] \qquad [4]$$

where $\mathbf{s}_i$ denotes ith row of the class matrix **S**, and E denotes operator of the mathematical expectations. When both sides in equation 4 are multiplied by unknown extended basis matrix $\overline{\mathbf{A}}$ it is obtained

$$\tilde{\overline{\mathbf{X}}} = \overline{\mathbf{A}}\tilde{\mathbf{S}} \qquad [5]$$

where in the comparison with equation 3 operator T has been substituted by notation '~', i.e. $T[\overline{\mathbf{X}}] = \tilde{\overline{\mathbf{X}}}$ and $T[\mathbf{S}] = \tilde{\mathbf{S}}$. Innovations representation of the multispectral image 3 is in practice realized though application of the prediction-error filter on multispectral image 2. Prediction-error filter is estimated by means of the Levinson algorithm. Details can be found in: S. J. Orfanidis. Optimum Signal Processing – An Introduction, 2nd ed. MacMillan Publishing Comp., New York, 1988.

[0041] When in accordance with drawing 3 and paragraphs [0034]- [0040] multispectral image 1 has been transformed into multispectral image 3, the ICA algorithms are applied to multispectral image 3 in order to estimate the extended basis matrix $\overline{\mathbf{A}}$ or its inverse $\overline{\mathbf{A}}^{-1}$. The ICA algorithms perform this estimation in a way to minimize a functional $F\left(\overline{\mathbf{A}}^{-1}\tilde{\overline{\mathbf{X}}}, \overline{\mathbf{A}}\right)$ that represents measure of statistical independence among the non-Gaussian processes

$\widetilde{\mathbf{S}} = \overline{\mathbf{A}}^{-1}\widetilde{\overline{\mathbf{X}}}$. More details about the techniques for construction of the functional F and associated ICA algorithms can be found in the references cited in the existing state-of-the-art, paragraph [0022]. Multispectral image 2 is multiplied by estimated inverse of the extended basis matrix $\overline{\mathbf{A}}^{-1}$ in order to estimate the unknown class matrix $\mathbf{S} = \overline{\mathbf{A}}^{-1}\overline{\mathbf{X}}$. For a final selection of the class of interest form the unknown class matrix **S** additional criteria are used such as predictability, smoothness or sparseness. This depends on the *a priroi* knowledge of the dimensions of the class of interest relative to the dimensions of the multispectral image (1).

[0042] Drawings 4 schematically illustrate the case of spectrally similar and spectrally different classes $\mathbf{s}_1$ and $\mathbf{s}_2$ in the appropriate spatial visualisation. Drawing 4A: classes $\mathbf{s}_1$ and $\mathbf{s}_2$ are spectrally very similar. Drawing 4B: classes $\mathbf{s}_1$ and $\mathbf{s}_2$ are spectrally different. By convention we shall assume that class $\mathbf{s}_1$ represents healthy tissue, and class $\mathbf{s}_2$ represents tumour.

[0043] Drawing 5 schematically illustrates the case of spectrally similar and spectrally different classes $\mathbf{s}_1$ and $\mathbf{s}_2$ in the wavelength region. Shown are spectral responses of the pixels located in the regions of classes $\mathbf{s}_1$ and $\mathbf{s}_2$ according to drawing 4. In the adopted designation systems B denotes spectral component that corresponds with the blue colour, G denotes spectral component that corresponds with the green colour, and R denotes spectral component that correspond with the red colour. In two-spectral resolution B-R classes $\mathbf{s}_1$ and $\mathbf{s}_2$ are spectrally very similar or even identical what corresponds with a drawing 4A. In three-spectral resolution B-G-R classes $\mathbf{s}_1$ and $\mathbf{s}_2$ are spectrally different what corresponds with a drawing 4B. Equivalence of the three-spectral B-G-R resolution can be obtained by application of the transformation for nonlinear dimensionality expansion and innovations representation to B-G image in two-spectral resolution. This yields effect shown in drawing 4B.

[0044] Drawing 6 schematically illustrates the case of spectrally similar and spectrally different classes $\mathbf{s}_1$ and $\mathbf{s}_2$ in the appropriate coordinate systems. Drawing 6A: two-spectral resolution, two-dimensional B-R system, spectral vectors of the classes $\mathbf{s}_1$ and $\mathbf{s}_2$ are collinear. Drawing 6B: three-spectral resolution, three-dimensional B-G-R system, spectral vectors of the classes $\mathbf{s}_1$ and $\mathbf{s}_2$ are spread. Equivalence of the three-spectral B-G-R resolution can be

obtained by application of the transforms for nonlinear dimensionality expansion and innovations representation to an image in two-spectral B-G resolution. This yields an effect illustrated in drawing 4B.

[0045] Drawing 7 schematically illustrates quality of the visual contrast of the spatial maps of the healthy tissue $\mathbf{s}_1$ and tumour $\mathbf{s}_2$ extracted by direct application of the ICA algorithms to multispectral image 1, as an example two-spectral image 4A. By convention black colour means class existence while white colour means class absence. Drawing 7A: extracted spatial map of the healthy tissue. Drawing 7B: extracted spatial map of the tumour. Visual contrast of the extracted spatial maps is poor.

[0046] Drawing 8 schematically illustrates quality of the visual contrast of the spatial maps of the healthy tissue $\mathbf{s}_1$ and tumour $\mathbf{s}_2$ extracted by applications of the ICA algorithms to the innovations representation of the multispectral image 3. Multispectral image 3 is obtained by application of the nonlinear transform for dimensionality expansion and linear transformation for innovations representation to multispectral image 1, as an example two-spectral image 4A. By convention black colour means class existence while white colour means class absence. Drawing 8A shows extracted spatial map of the healthy tissue. Drawing 8B shows extracted spatial map of the tumour. Visual contrast of the extracted spatial maps is good.

[0047] Drawings 9A and 9B respectively show skin tumour with the high level and low level of fluorescence. As it is evident in Figure 9B the demarcation line of the tumour is hardly visible i.e. the visual contrast is very poor.

[0048] Drawings 10A and 10B respectively show demarcation line of the tumour extracted by the proposed invention. Drawing 10A is obtained by application of the invention to drawing 9A. Drawing 10B is obtained by application of the invention to drawing 9B. It is evident that proposed invention extracts approximately the same demarcation line in both cases. This demonstrates its robustness with respect to the variability of intensity level of the fluorescent image.

[0049] Drawings 11A and 11B respectively show demarcation line of the tumour extracted by the ratio imaging method according to the existing state-of-the-art, from drawings 9A and 9B.

The threshold value was 5. Small effects of the variation of the intensity level of the fluorescence are visible in drawings 11B.

[0050] Drawings 12A and 12B respectively show demarcation line of the tumour extracted by the ratio imaging method according to the existing state-of-the-art, from drawings 9A and 9B. The threshold value was 10. Effects of the variation of the intensity level of the fluorescence are clearly visible on drawing 12B when threshold value has been set tp 10. Because the optimal value of the threshold depends on the intensity of the illuminating light, concentration level of the photo sensitizer and time duration of the treatment of the tumour by means of the photo sensitizer, it is clear that the ratio imaging is very sensitive on the variability of these parameters.

[0051] Invention can also be applied to suppress reflected illumination in the multiple fluorescence based photodynamic therapy systems. It is characteristic for such systems that fluorescence induced by one illumination is superimposed with reflections of another illumination. Because radiations spectrally overlap, it can be expected that they are statistically partially dependent. By application of the proposed invention it is possible to achieve higher suppression level of the reflected radiation than when ICA algorithms are directly used for the same purpose.

[0052] Proposed invention can be additionally applied during tumour surgery by estimating tumour boundaries in real time. This eliminates necessity to performing a biopsy on the tissue sample and waiting for the outcome during the surgery in order to asses the tumour boundaries. The invention can also be applied to segmentation of the multispectral fluorescent image of the tissue 1 acquired when the time interval of the treatment of the tumour with the photo sensitizer is shortened or when the concentration of the photo sensitizer is reduced. Prpoposed invetion is applied to unsupervised segmentation of the multispectral fluorescent image 1 acquired under reduced intensity of the illuminating light, that becomes especially imporant for the surgery of the brain tumour and for the monitoring of the therapy.

CLAIMS

1. Method for real time visualisation and demarcation of tumours by means of photodynamic method and analysis of the fluorescent multispectral image **comprising** following steps:
- recording of the fluorescent image (1) by multispectral camera (6) where fluorescent image (1) is represented by the linear combination of the unknown classes **S**,
- transformation of fluorescent multispectral image into new multispectral image (2) by using nonlinear dimensionality expansion,
- linear transformation of the multispectral image (2) with extended dimensionality,
- independent component analysis of the innovation representation of the multispectral image (3) that is result of the transformations of the fluorescent multispectral image (1) and multispectral image (2),
- extraction of the tumour map or class of interest according to the chosen criterion, and
- visualisation of the tumour.
2. Method as claimed in claim 1, **characterized by,** that transformation of the fluorescent multispectral image consist of spectral components of the multispectral fluorescent image (1) and generated spectral images of the second order that encompass linear and nonlinear correlations and cross-correlations contained in multispectral image (1).
3. Method as claimed in claim 2, **characterized by**, that generation of the spectral images of the second order is carried out by taking the second power of the spectral components x_i of the multispectral image (1) and by mutual multiplication $x_i x_j$ of the spectral components of the multispectral fluorescent image (1).
4. Method as claimed in claim 2, **characterized by**, that dimensionality of multispectral image is additionally increased through generation of the nonlinearly correlated spectral images by calculating square root of the spectral components x_i of the multispectral fluorescent image (1).
5. Method as claimed in claim 1, **characterized by** that linear transformation of the multispectral image (2) with extended dimensionality is carried out by transforming multispectral image (2) with extended dimensionality into innovations representation of the multispectral image (3).

6. Method as claimed in claim 5, **characterized by**, that transformation into innovations representation of the multispectral image (3) is implemented by the prediction-error filter of the multispectral image (2) with extended dimensionality by means of Levinson algorithm.
7. Method as claimed in claims 5 and 6, **characterized by**, that innovation representations $\widetilde{\mathbf{S}}$ of the unknown classes are more statistically independent and more non-Gaussian than unknown classes **S**.
8. Method as claimed in claim 1, **characterized by**, that independent component analysis algorithms are applied to innovation representations of the multispectral image (3) that is result of the transformation of fluorescent image (1) and multispectral image (2) to reconstruct the unknown basis matrix $\overline{\mathbf{A}}$ or its inverse $\overline{\mathbf{A}}^{-1}$ with the aim to estimate the unknown classes **S**.
9. Method as claimed in any of the previous claims, **characterized by**, that multispectral image (2) with extended dimensionality is multiplied by the estimated inverse of the extended basis matrix $\overline{\mathbf{A}}^{-1}$.
10. Method as claimed in any of the previous claims, **characterized by,** that extraction of the tumour map or class of interest according to the chosen criterion is carried out from the reconstructed matrix of the unknown classes **S** where additional criteria are used such as measures of predictability, smoothness or sparseness in dependence on the *a priori* assumed spatial dimensions of the class of interest relative to the spatial size of the multispectral image (1).
11. Method as claimed in any of the previous claims, **characterized by,** that class of interest is either surface or sub-surface tumour.
12. Method as claimed in any of the previous claims, **characterized by,** that class of interest is any type of the unhealthy tissue.
13. Method as claimed in any of the previous claims, **characterized by,** that it is applied to visualisation and spatial demarcation of various types of surface or sub-surface tumours or unhealthy tissue by means of the unsupervised segmentation of the fluorescent multispectral image of the tissue 1 recorded with reduced concentration of the photo sensitizer or with reduced intensity of the illuminating light or with reduced duration of the treatment by photo sensitizer.
14. Method as claimed in claim 13, **characterized by,** that it is applied to the visualisation and spatial demarcation of the various types of surface and sub-surface tumours or

unhealthy tissue during real time estimation of the tumour boundaries or during monitoring of the therapy.

AMENDED CLAIMS

received by the International Bureau on 4 June 2008 (04.06.2008)

CLAIMS

1. Method for real time visualisation and demarcation of tumours by means of fluorescent marking and analysis of the fluorescent multispectral image **comprising** following steps:
- recording of the fluorescent image (1) by multispectral camera (6) where fluorescent image (1) is represented by the linear combination of the unknown classes **S**,
- transformation of fluorescent multispectral image into new multispectral image (2) by using nonlinear dimensionality expansion,
- linear transformation of the multispectral image (2) with extended dimensionality,
- independent component analysis of the innovation representation of the multispectral image (3) that is result of the transformations of the fluorescent multispectral image (1) and multispectral image (2),
- extraction of the tumour map or class of interest according to the chosen criterion, and
- visualisation of the tumour.
2. Method as claimed in claim 1, **characterized by,** that transformation of the fluorescent multispectral image consist of spectral components of the multispectral fluorescent image (1) and generated spectral images of the second order that encompass linear and nonlinear correlations and cross-correlations contained in multispectral image (1).
3. Method as claimed in claim 2, **characterized by**, that generation of the spectral images of the second order is carried out by taking the second power of the spectral components x_i of the multispectral image (1) and by mutual multiplication $x_i x_j$ of the spectral components of the multispectral fluorescent image (1).
4. Method as claimed in claim 2, **characterized by**, that dimensionality of multispectral image is additionally increased through generation of the nonlinearly correlated spectral images by calculating square root of the spectral components x_i of the multispectral fluorescent image (1).
5. Method as claimed in claim 1, **characterized by** that linear transformation of the multispectral image (2) with extended dimensionality is carried out by transforming multispectral image (2) with extended dimensionality into innovations representation of the multispectral image (3).

Statement under Article 19(1)

The following sheets are replaced:

Claims: page 22

Differences between the replaced sheets

Page 22

Claim 1 is amended

Claims 2-5 remain unchanged

Examiner stated that claim 1 as filed originally can be interpreted ambiguously since the phrase "photodynamic method" could be interpreted as photodynamic method or therapy.

Accordingly, for better defining of the invention and avoiding any vagueness, the applicant has amended claim 1 in a way to replace phrase "photodynamic method" with "fluorescent marking".

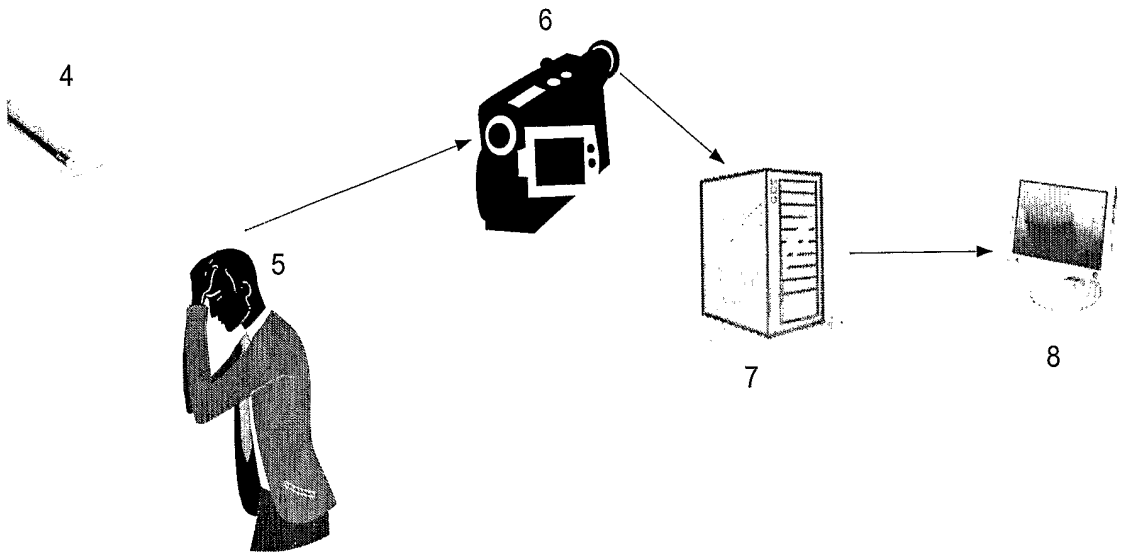

Drawing 1.

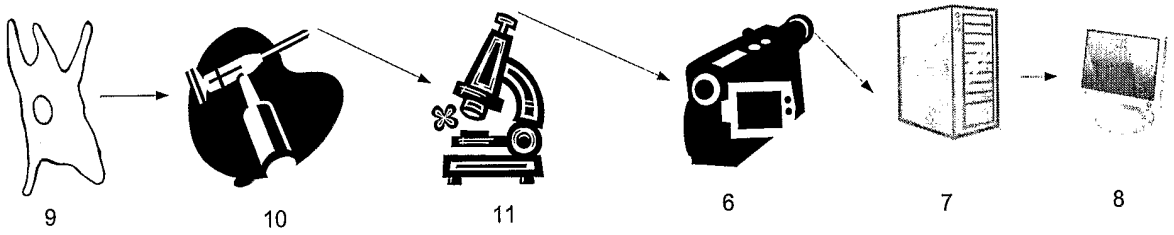

Drawing 2.

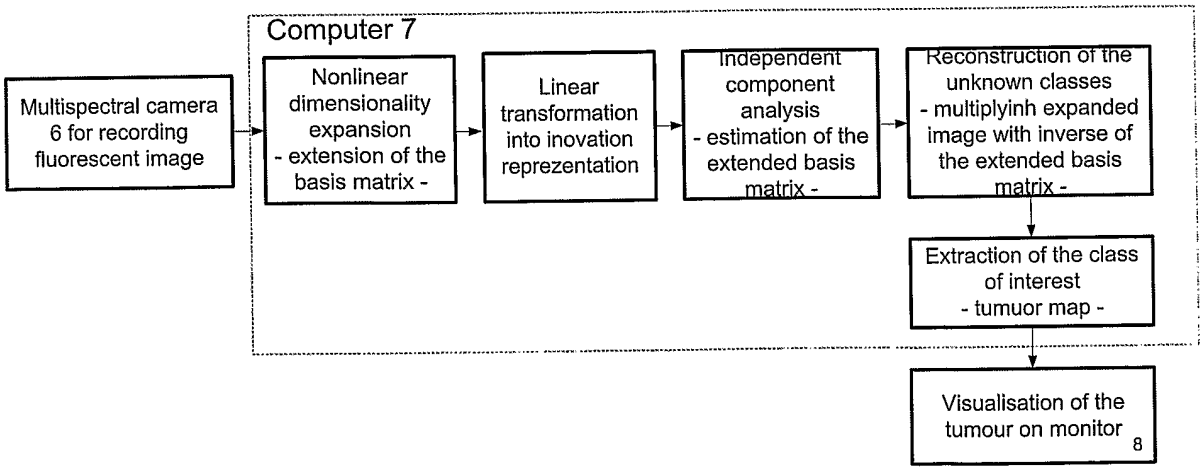

Drawing 3.

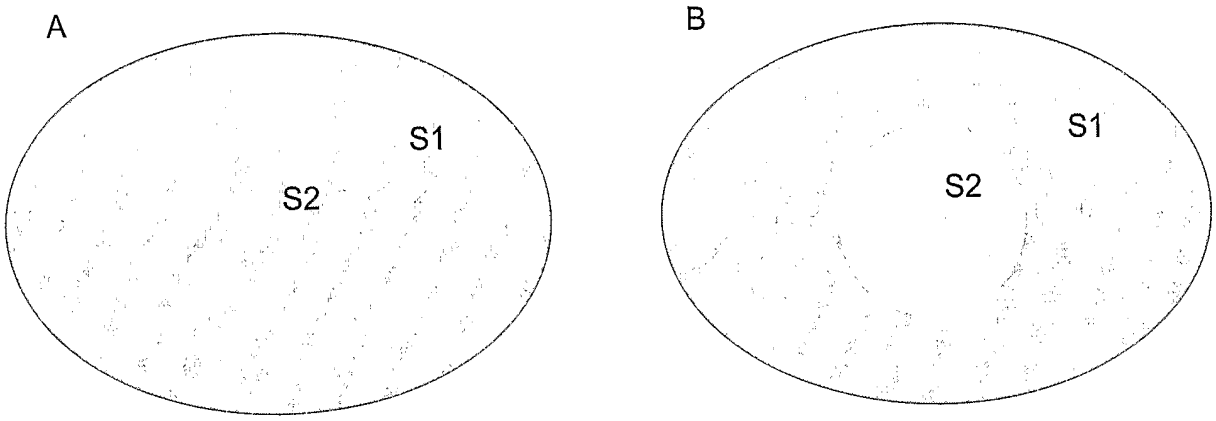

Drawing 4 A and B

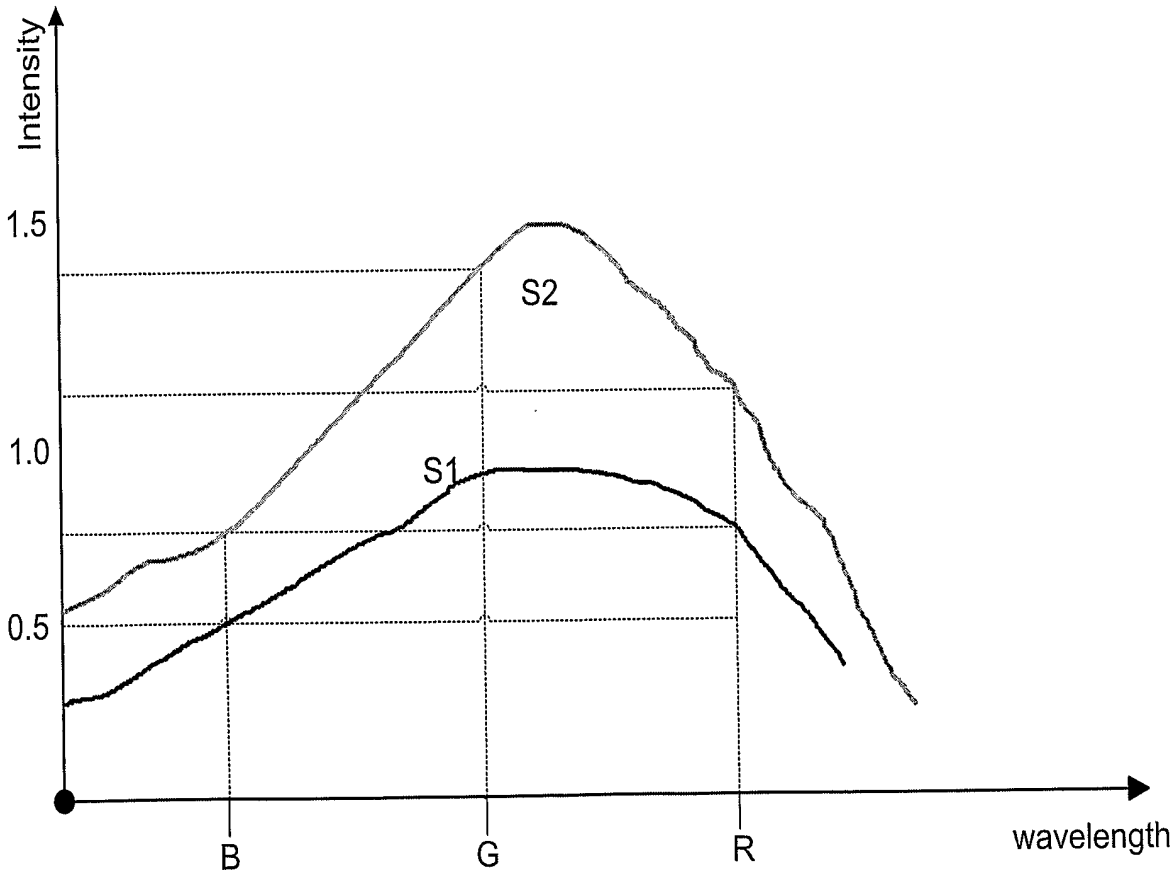

Drawing 5.

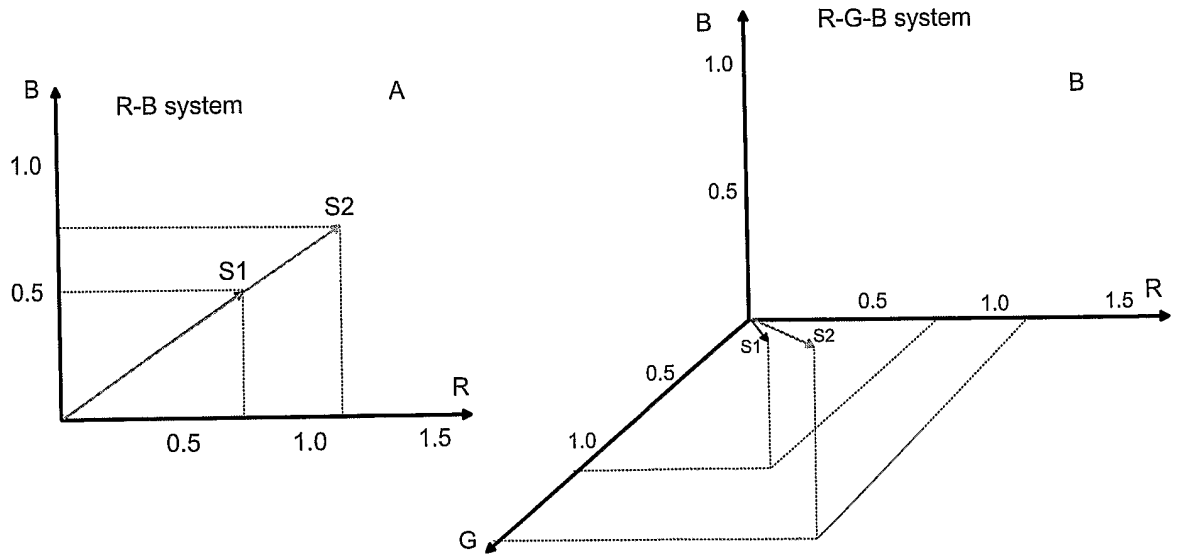

Drawing 6 A and B.

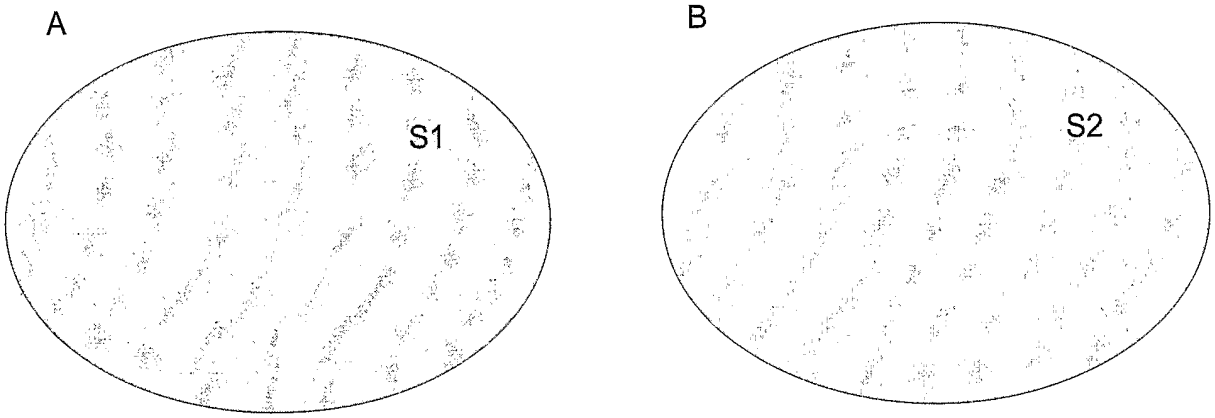

Drawing 7 A and B.

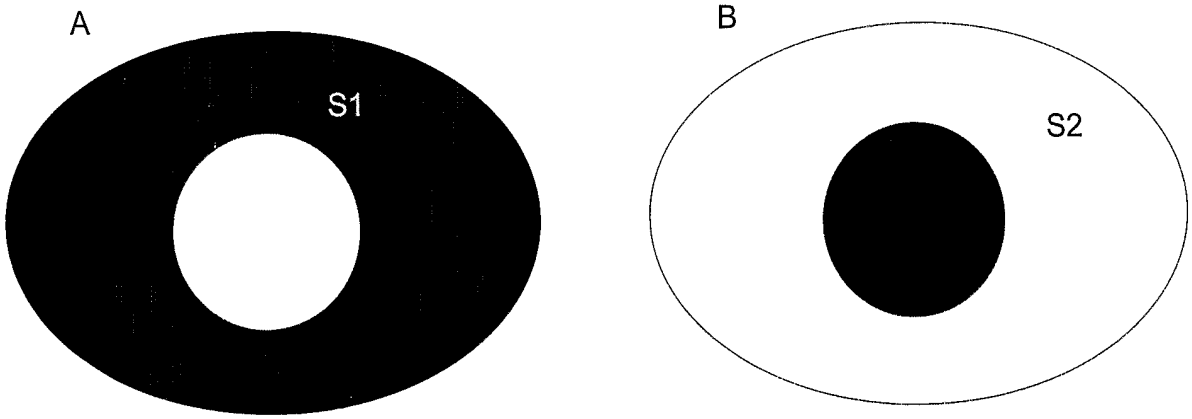

Drawing 8 A and B.

A

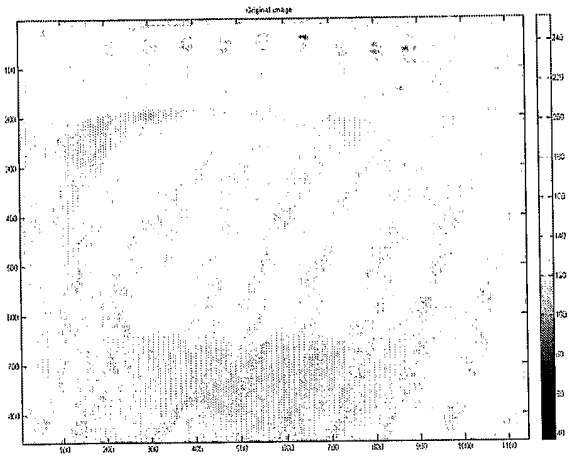

B

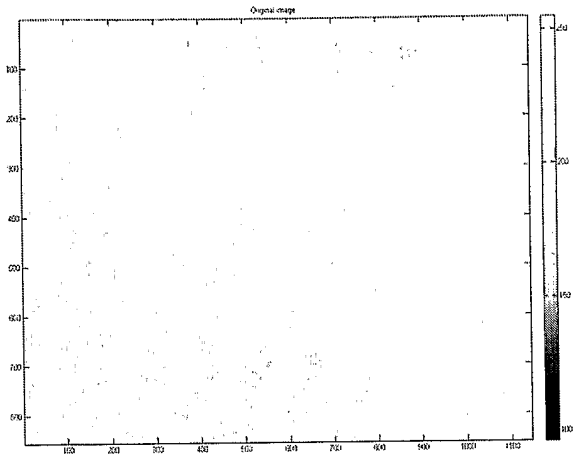

Drawing 9 A and B.

A

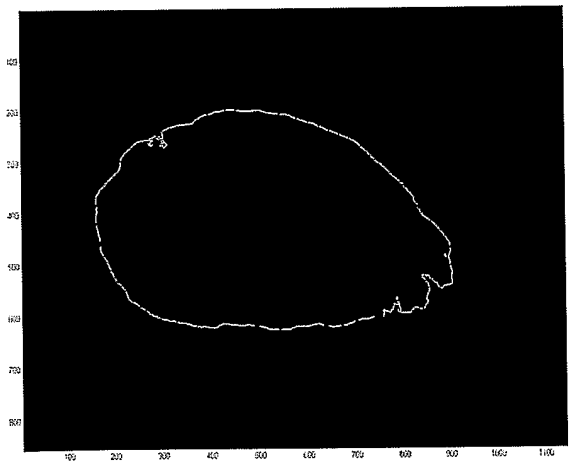

B

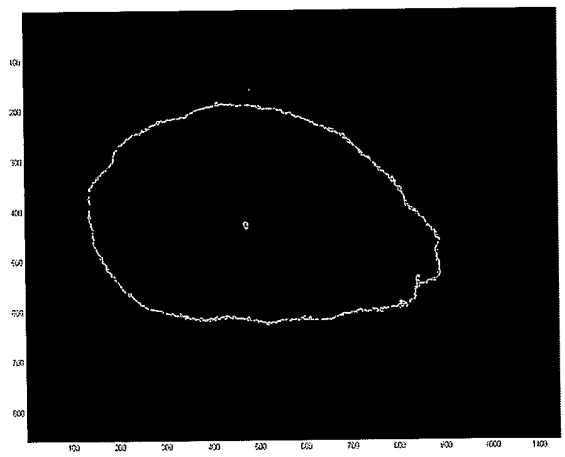

Drawing 10 A and B.

A

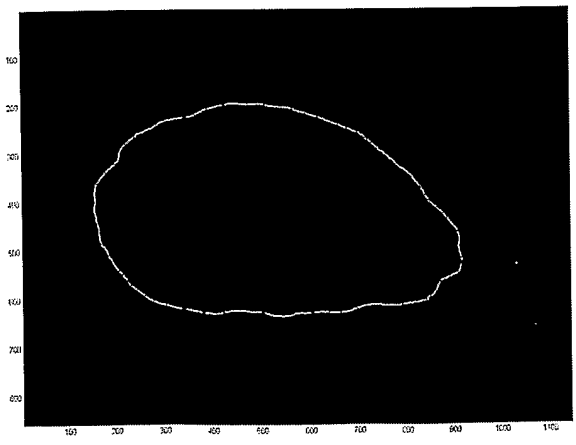

B

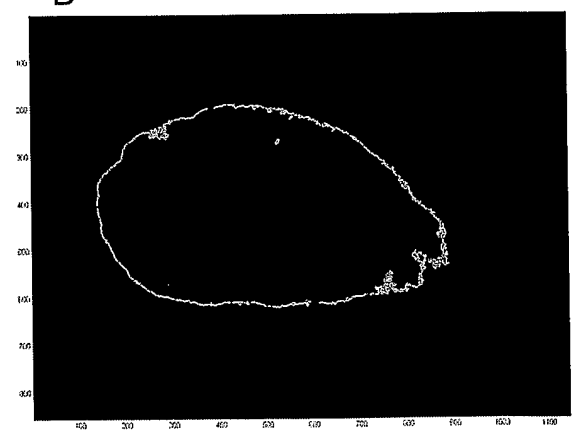

Drawing 11.

A

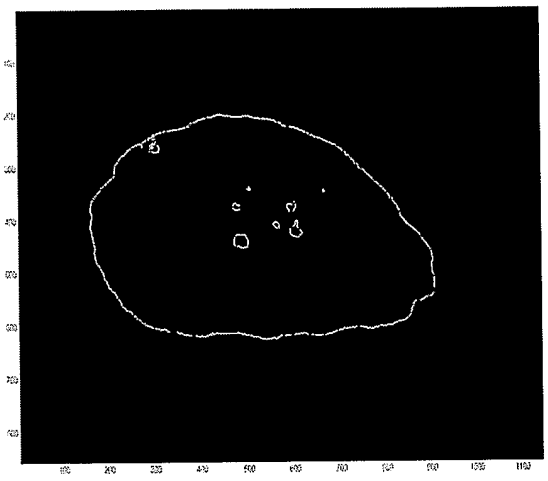

B

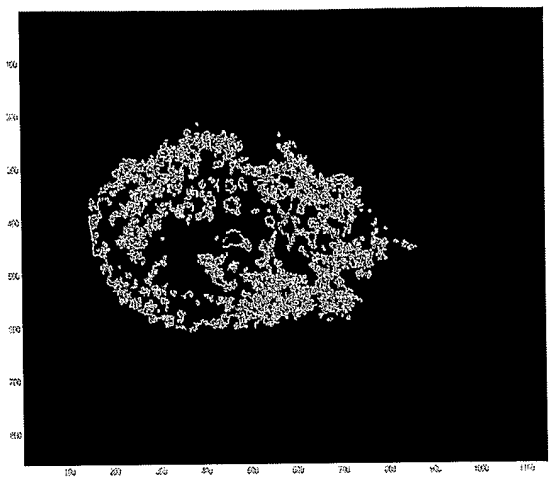

Drawing 12 A and B.

INTERNATIONAL SEARCH REPORT

International application No
PCT/HR2007/000013

A. CLASSIFICATION OF SUBJECT MATTER
INV. A61B5/00 G01N21/64

According to International Patent Classification (IPC) or to both national classification and IPC

B. FIELDS SEARCHED

Minimum documentation searched (classification system followed by classification symbols)
G01N

Documentation searched other than minimum documentation to the extent that such documents are included in the fields searched

Electronic data base consulted during the international search (name of data base and, where practical, search terms used)
EPO-Internal

C. DOCUMENTS CONSIDERED TO BE RELEVANT

Category*	Citation of document, with indication, where appropriate, of the relevant passages	Relevant to claim No.
A	ANDERSSON-ENGELS S ET AL; "MEDICAL DIAGNOSTIC SYSTEM BASED ON SIMULTANEOUS MULTISPECTRAL FLUORESCENCE IMAGING" APPLIED OPTICS, OSA, OPTICAL SOCIETY OF AMERICA, WASHINGTON, DC, US, vol. 33, no. 34, 1 December 1994 (1994-12-01), pages 8022-8029, XP000485544 ISSN: 0003-6935 page 8023, right-hand column, line 1 - page 8027, left-hand column, line 3 figures 1-5 ----- -/--	1

[X] Further documents are listed in the continuation of Box C.

[X] See patent family annex.

* Special categories of cited documents :

"A" document defining the general state of the art which is not considered to be of particular relevance

"E" earlier document but published on or after the international filing date

"L" document which may throw doubts on priority claim(s) or which is cited to establish the publication date of another citation or other special reason (as specified)

"O" document referring to an oral disclosure, use, exhibition or other means

"P" document published prior to the international filing date but later than the priority date claimed

"T" later document published after the international filing date or priority date and not in conflict with the application but cited to understand the principle or theory underlying the invention

"X" document of particular relevance; the claimed invention cannot be considered novel or cannot be considered to involve an inventive step when the document is taken alone

"Y" document of particular relevance; the claimed invention cannot be considered to involve an inventive step when the document is combined with one or more other such documents, such combination being obvious to a person skilled in the art.

"&" document member of the same patent family

Date of the actual completion of the international search	Date of mailing of the international search report
25 April 2008	15/05/2008

Name and mailing address of the ISA/	Authorized officer
European Patent Office, P.B. 5818 Patentlaan 2 NL – 2280 HV Rijswijk Tel. (+31–70) 340–2040, Tx. 31 651 epo nl, Fax: (+31–70) 340–3016	Chen, Amy

INTERNATIONAL SEARCH REPORT

International application No
PCT/HR2007/000013

C(Continuation). DOCUMENTS CONSIDERED TO BE RELEVANT

Category*	Citation of document, with indication, where appropriate, of the relevant passages	Relevant to claim No.
A	SIEGEL ET AL.: "Whole-field five-dimensional fluorescence microscopy combining lifetime and spectral resolution with optical sectioning" OPTICS LETTERS, vol. 26, no. 17, 1 September 2001 (2001-09-01), pages 1338-1340, XP002478141 US the whole document	1
A	WO 2005/040739 A (SOFTMAX INC [US]; VISSER ERIK [US]; JUNG TZYY-PING [US]; CHAN KWOKLEUN) 6 May 2005 (2005-05-06) paragraph [0037] - paragraph [0044] paragraph [0049] - paragraph [0054] paragraph [0059] - paragraph [0067] figures 1-6	1
A	DU ET HOWARD: "Multispectral image classification using idependent component analysis and data dimentionality expansion apporaches" PROCEEDINGS OF SPIE, vol. 5546, 2004, pages 374-381, XP002478142 Bellingham, US abstract page 374, line 1 - page 377, line 28	1
A	OKIMOTO ET AL.: "New features for detecting cervical pre-cancer using hyperspectral diagnostic imaging" PROCEEDINGS OF THE SPIE, vol. 4255, 2001, pages 67-79, XP002478143 US page 68, line 19 - page 72, line 22	1

INTERNATIONAL SEARCH REPORT

Information on patent family members

International application No
PCT/HR2007/000013

Patent document cited in search report	Publication date	Patent family member(s)	Publication date
WO 2005040739 A	06-05-2005	EP 1680650 A2	19-07-2006